

**Naval Research Laboratory**

Washington, DC 20375-5000



---

**NRL Report 9107**

**Pulse Compression Degradation Due to Open  
Loop Adaptive Cancellation, Part I**

KARL GERLACH

*Target Characteristics Branch  
Radar Division*

July 31, 1991

Approved for public release; distribution unlimited.

# REPORT DOCUMENTATION PAGE

*Form Approved*  
*OMB No. 0704-0188*

Public reporting burden for this collection of information is estimated to average 1 hour per response, including the time for reviewing instructions, searching existing data sources, gathering and maintaining the data needed, and completing and reviewing the collection of information. Send comments regarding this burden estimate or any other aspect of this collection of information, including suggestions for reducing this burden, to Washington Headquarters Services, Directorate for Information Operations and Reports, 1215 Jefferson Davis Highway, Suite 1204, Arlington, VA 22202-4302, and to the Office of Management and Budget, Paperwork Reduction Project (0704-0188), Washington, DC 20503.

<b>1. AGENCY USE ONLY (Leave blank)</b>		<b>2. REPORT DATE</b> July 31, 1991	<b>3. REPORT TYPE AND DATES COVERED</b>	
<b>4. TITLE AND SUBTITLE</b> Pulse Compression Degradation Due to Open Loop Adaptive Cancellation, Part I			<b>5. FUNDING NUMBERS</b>  PE - 62111N PR - RA11W51,2559	
<b>6. AUTHOR(S)</b>  Karl Gerlach			<b>8. PERFORMING ORGANIZATION REPORT NUMBER</b>  NRL Report 9107	
<b>7. PERFORMING ORGANIZATION NAME(S) AND ADDRESS(ES)</b>  Naval Research Laboratory Washington, DC 20375-5000			<b>10. SPONSORING / MONITORING AGENCY REPORT NUMBER</b>	
<b>9. SPONSORING / MONITORING AGENCY NAME(S) AND ADDRESS(ES)</b>  Office of Naval Technology Arlington, VA 22217			<b>11. SUPPLEMENTARY NOTES</b>	
<b>12a. DISTRIBUTION / AVAILABILITY STATEMENT</b>  Approved for public release; distribution is unlimited.			<b>12b. DISTRIBUTION CODE</b>	
<b>13. ABSTRACT (Maximum 200 words)</b>  Performance results for the sidelobe level of a compressed pulse that has been preprocessed through an adaptive canceller are obtained. The adaptive canceller is implemented using the Sampled Matrix Inversion (SMI) algorithm. Because of finite sampling, the quiescent compressed pulse sidelobe levels are degraded because of the preprocessing of the main channel input data stream (the uncompressed pulse) through an adaptive canceller. If $N$ is the number of input canceller channels (main and auxiliaries) and $K$ is the number of independent samples per channel, then it is shown that $K/N$ can be significantly greater than one in order to retain sidelobes that are close to the original quiescent sidelobe level (with no adaptive canceller). Also, it is shown that the maximum level of degradation is independent of whether pulse compression occurs before or after the adaptive canceller if the uncompressed pulse is completely contained within the $K$ samples that are used to calculate the canceller weights. Furthermore, this same analysis can be used to predict the canceller noise power level that is induced by having the desired signal present in the canceller weight calculation.				
<b>14. SUBJECT TERMS</b> Gram-Schmidt Adaptive filter Radar			<b>15. NUMBER OF PAGES</b> 31	
ECCM Adaptive cancellation			<b>16. PRICE CODE</b>	
<b>17. SECURITY CLASSIFICATION OF REPORT</b> UNCLASSIFIED	<b>18. SECURITY CLASSIFICATION OF THIS PAGE</b> UNCLASSIFIED	<b>19. SECURITY CLASSIFICATION OF ABSTRACT</b> UNCLASSIFIED	<b>20. LIMITATION OF ABSTRACT</b> SAR	

## CONTENTS

1. INTRODUCTION .....	1
2. THE GS CANCELLER .....	2
3. SIGNAL MODEL .....	6
4. GS SIMPLIFICATIONS .....	9
5. SINGLE AUXILIARY CROSS-CORRELATIONS .....	13
6. MULTIPLE AUXILIARY CROSS-CORRELATIONS .....	15
7. SIDELobe DEGRADATION DERIVATION .....	18
8. RESULTS .....	20
9. SUMMARY .....	23
REFERENCES .....	23
APPENDIX — Derivation of Eqs. (35)-(36) .....	25

# PULSE COMPRESSION DEGRADATION DUE TO OPEN LOOP ADAPTIVE CANCELLATION, PART I

## 1. INTRODUCTION

An adaptive canceller [1] adjusts the auxiliary channel settings so as to null out interference in the main channel (Fig. 1). The weights of the auxiliary channels are adjusted to minimize the output noise power residue. If the noise environment is not known a priori, these weight settings must be estimated from a finite set of incoming data on the input channels. Thus, the weight settings will have perturbations about the quiescent optimum weight settings. These perturbations cause, for example, the output noise power residue to rise [1-4], and if the adaptive canceller is used in the sidelobe antenna canceller configuration, the adaptive array antenna sidelobe level to increase [5].

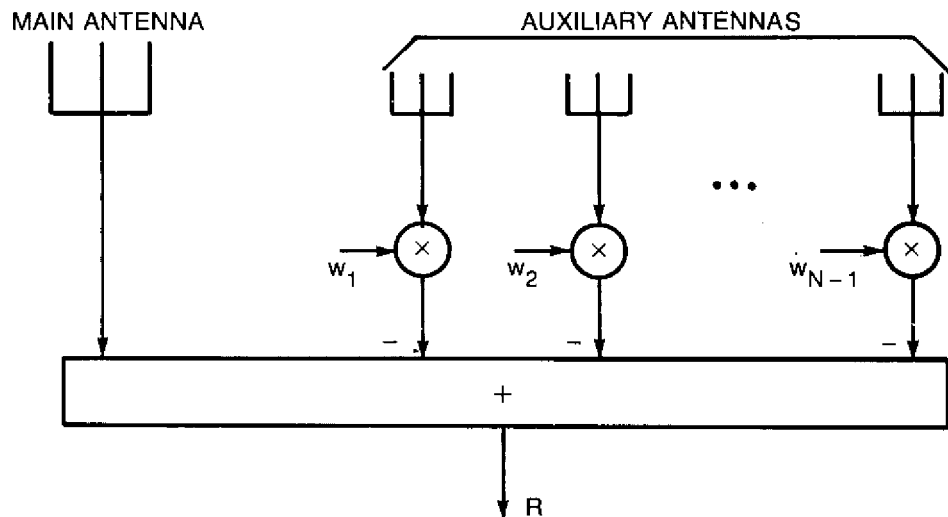


Fig. 1 — Adaptive canceller

A pulse compressor is essentially the matched filter for a given radar waveform. Most of the energy in the received radar waveform is compressed into a given single-range cell and, thus, the signal level can be increased significantly for detection purposes. However, some energy does leak into the sidelobes of the compressed pulse response, resulting in low gain in range cells outside of the given range cell. If a target or piece of clutter is large enough, it can break through and be detected in these range sidelobes, falsely indicating a target detection or masking a real target. Thus, it is highly desirable to maintain a low sidelobe response.

For the radar designer there is the choice of where to put the pulse compressor: before or after the canceller. A disadvantage of placing it before the canceller is that a pulse compressor must be placed in each antenna channel (main and auxiliaries) to maintain channel match. Another disadvantage is that the pulse compressor must have the dynamic range of the interference (possibly clutter and jamming) which has yet to be cancelled. These disadvantages do not exist if the pulse compressor is placed after the canceller. However, a disadvantage of placing the pulse compressor after the canceller is that the range sidelobe levels of the compressed pulse increase because a finite number of samples is used to compute the canceller weights. (We assume that the canceller weights are estimated from a block of input data and applied back onto the same input data set.) Hence, the designed radar waveform pulse compressor responses may not be achieved because of the interaction of the canceller with the pulse compressor. Because of the higher sidelobes, unwanted targets may break through and be detected. Significantly, as it will be shown, the maximum sidelobe levels that result from interacting with the canceller are independent of whether the input waveform was compressed before or after the canceller if the uncompressed pulse is completely contained within the samples that are used to calculate the canceller weights.

This report considers the degradations that result when trying to match-filter or pulse-compress a desired radar waveform after it has been processed through a particular adaptive canceller called the Sampled Matrix Inversion (SMI) algorithm [2]. The SMI algorithm is an open-loop, rapidly converging adaptive canceller implementation whose noise power convergence rate is independent of the external noise environment. For many years, it has been considered a baseline for fast converging adaptive canceller algorithms. The Gram-Schmidt (GS) canceller [4, 6-8] is a numerically equivalent implementation (assuming infinite accuracy) of the SMI algorithm with excellent performance simultaneously in arithmetic efficiency, stability, and convergence. In addition, it is a good analytical tool [4,5] with which to investigate the convergence properties of the SMI canceller. Because of the SMI's complexity, we assume that it is implemented digitally. Because the pulse compressor follows the canceller, we assume that it is also implemented digitally.

This report is laid out as follows. Section 2 briefly describes the GS canceller and Section 3 presents the signal model (for pulse compression). Some past results on GS cancellers are reviewed in Section 4. Sections 5 through 7 derive the analytical results and Section 8 discusses them.

For some applications, the matched filter is replaced by a filtering scheme that reduces the range sidelobes at the expense of signal gain at the matched point. Thus, a mismatched filter is used. It is shown that the results derived for the matched filter are applicable to the mismatched filter.

## 2. THE GS CANCELLER

Consider the general  $N$ -input Gram-Schmidt canceller structure as shown in Fig. 2. Let  $x_M(t)$ ,  $x_1(t)$ ,  $\dots$ ,  $x_{N-1}(t)$  represent the complex data signals in the 0th, 1st,  $\dots$ ,  $N-1$ th channels, respectively. We call the leftmost input  $x_M(t)$  the main channel and the remaining  $N-1$  inputs, the auxiliary channels. The main channel's signal consists of a desired signal plus additive noise (i.e., internal plus external noise). Cancellation of the signals from external interfering sources relies on the correlation of simultaneously received signals in the main and auxiliary channels. The internal noises on each channel are assumed to be uncorrelated between channels. The GS canceller decorrelates the auxiliary inputs one at a time from the other inputs by using the basic 2-input GS processor as is shown in Fig. 3. For example, Fig. 2 shows that  $x_{N-1}(t)$  is uncorrelated with  $x_M^{(2)}(t)$ ,  $x_1^{(2)}(t)$ ,  $\dots$ ,  $x_{N-2}^{(2)}(t)$  in the first level of decomposition. Next, the output channel that results from

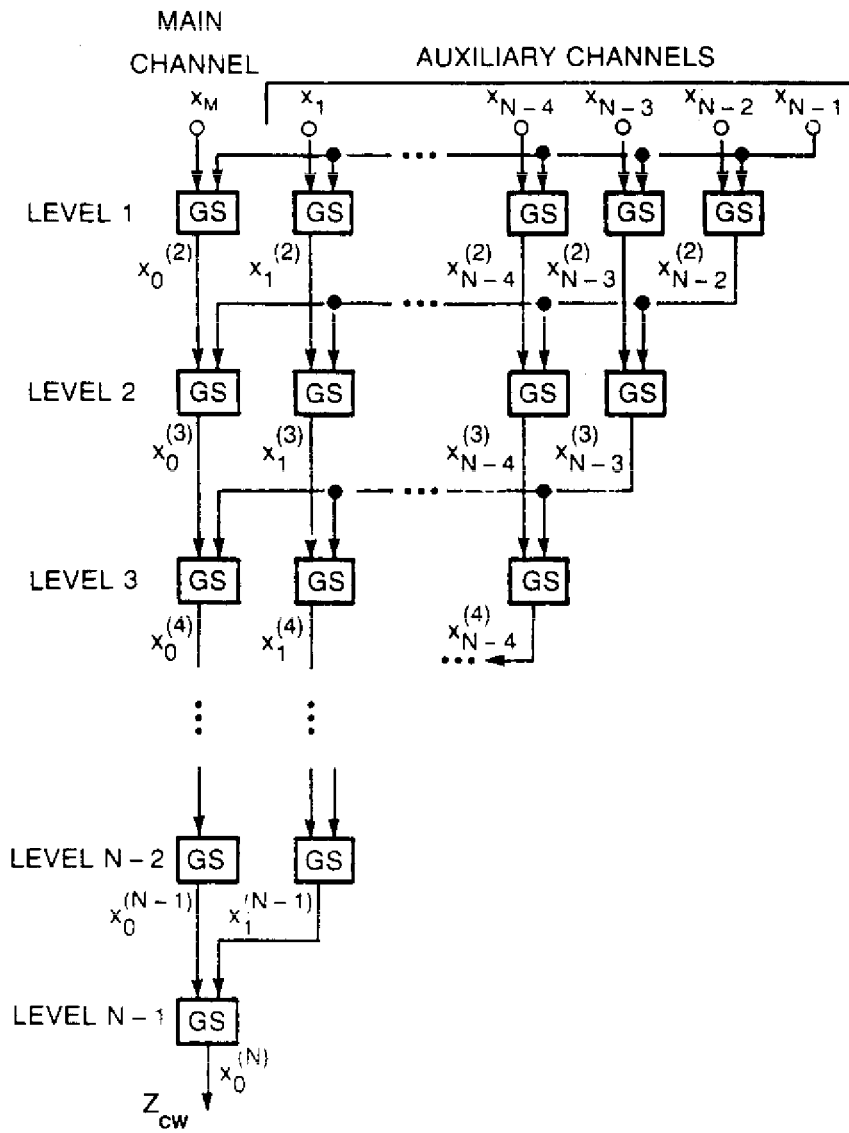


Fig. 2 — GS structure

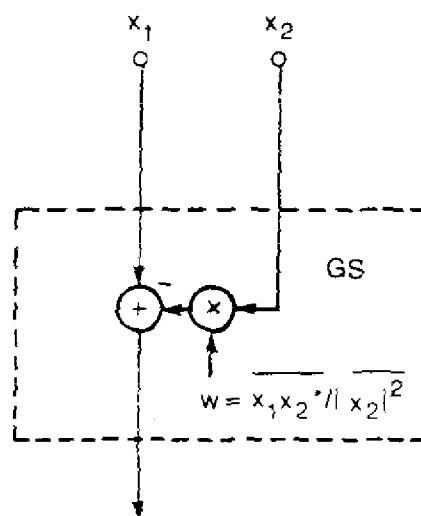


Fig. 3 — Basic 2-input GS canceller

decorrelating  $x_{N-1}(t)$  with  $x_{N-2}(t)$ , is decorrelated from the other outputs of the first-level GSs. The decomposition proceeds until a final output channel is generated. If the decorrelation weights in each of the 2-input GSs are computed from an infinite number of input samples, then the main output channel is totally decorrelated with the input:  $x_1(t), x_2(t), \dots, x_{N-1}(t)$ . Also,  $x_n^{(N-n)}(t)$ ,  $n = 0, 1, \dots, N - 1$  are pairwise statistically uncorrelated or orthogonal.

If an infinite number of input samples is not used then the decorrelation weights associated with each 2-input GS canceller are estimated by using finite averaging. One method of processing data through the GS canceller is called concurrent processing because the weights are estimated from a block of input data and applied back onto the same input data set. (For a discussion of other types of GS processing, see Ref. 4.) This type of processing is often necessary to handle blinking interference sources.

We briefly describe the concurrent GS canceller. Let  $x_n^{(m)}$  represent the outputs of the 2-input GSs on the  $(m - 1)$  level. Then outputs of the 2-input GSs at the  $m$ th level are given by

$$x_n^{(m+1)} = x_n^{(m)} - w_n^{(m)} x_{N-m}^{(m)} \quad \begin{matrix} n = 0, 1, \dots, N - m - 1 \\ m = 1, 2, \dots, N - 1 \end{matrix} \quad (1)$$

Note that  $x_n^{(1)} = x_n$ . The weight  $w_n^{(m)}$ , seen in Eq. (1), is computed so as to uncorrelate  $x_n^{(m+1)}$ ,  $n = 0, 1, \dots, N - m - 1$  with  $x_{N-m}^{(m)}$ . For  $K$  input samples per channel, this weight is estimated as

$$w_n^{(m)} = \frac{\sum_{k=1}^K x_{N-m}^{(m)*}(k) x_n^{(m)}(k)}{\sum_{k=1}^K |x_{N-m}^{(m)}(k)|^2}, \quad (2)$$

where  $*$  denotes the complex conjugate and  $|\cdot|$  is the magnitude. Here  $k$  indexes the sampled data.

Let  $x_0$  represent the additive noise in the main channel. For this development, we make the following five assumptions:

1. The  $x_0, x_1, \dots, x_{N-1}$  are identically distributed Gaussian complex random variables (r.v.).
2. These same r.v.s are samples from stationary processes with zero mean.
3.  $x_{n_1}(k_1)$  is statistically independent of  $x_{n_2}(k_2)$  for  $k_1 \neq k_2$ .
4. The desired signals are not present in the auxiliary channels.
5.  $K \geq N$ .

It is necessary to make the last assumption because for  $K < N - 1$  the GS canceller is numerically unstable because of the singularity of the estimated input covariance matrix, and for  $K = N - 1$  the output of a concurrent GS canceller is always zero [4]. In the following discussion, a normalized  $L$ -length multivariate complex circular Gaussian vector is defined to have  $L$  elements, each of which has real and imaginary parts that are independent Gaussian r.v.s with 0 mean and variance equal to  $1/2$  (the magnitude variance is one). In addition, the  $L$  elements are independent of one another.

Figure 4 presents simplified  $N$ -input GS canceller structures for concurrent processing. The notation  $GS_{K,N}$  indicates that an  $N$ -input GS structure uses  $K$  samples from each channel to compute the weights interior to the GS structure. The 0th channel (the far left channel in Fig. 2 or 4) is always designated as the main channel and the others are called the auxiliary channels (or just AUXs). Figure 5 represents the GS structure with  $N$  orthogonal outputs displayed.

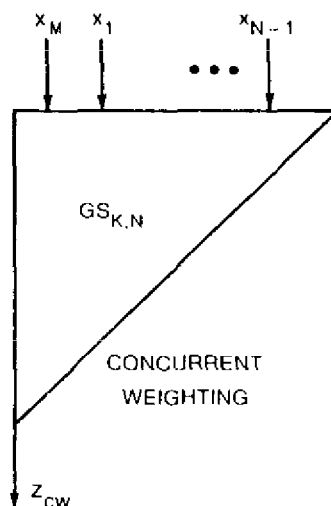


Fig. 4 — Representation of GS canceller with  $N$  channels and  $K$  samples per channel

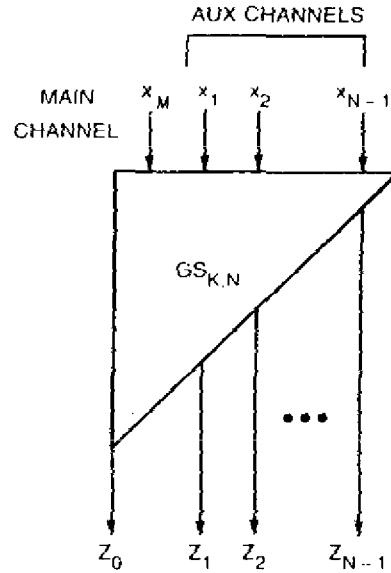


Fig. 5 — GS representation with  $N$  output channels

### 3. SIGNAL MODEL

A network whose frequency response function maximizes the output peak signal-to-mean noise power ( $S/N$ ) ratio is called a matched filter. Almost all radar receivers are designed by using the matched filter criteria. If  $h(t)$  is the impulse response function of the matched radar receiver,  $s(t)$  is the transmitted radar waveform, and the noise interference is white and additive, then it can be shown [9-11] that

$$h(t) = s^*(-t), \tag{3}$$

where  $*$  denotes the complex conjugate operation.

A sampled matched receiver design is based on the same principle of maximizing  $S/N$ . We sample the transmitted radar waveform at equal time intervals  $\tau$ . Let  $s_1, s_2, \dots, s_L$  be the values of the sampled transmitted waveform or code where  $L$  is the number of sampled points (Fig. 6). Set

$$\mathbf{s} = (s_1, s_2, \dots, s_L)^T, \tag{4}$$

where  $T$  denotes the vector transpose operation. The sampled receiver applies a weighting vector  $\mathbf{g} = (g_1, g_2, \dots, g_L)^T$  such that

$$y = \mathbf{g}^T \mathbf{s}. \tag{5}$$

It can be shown that ( $S/N$ ) is maximized when

$$\mathbf{g} = \mathbf{s}^*. \tag{6}$$

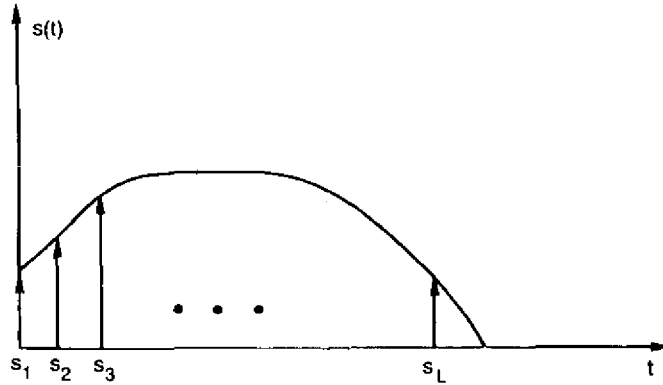


Fig. 6 — Sample radar waveform

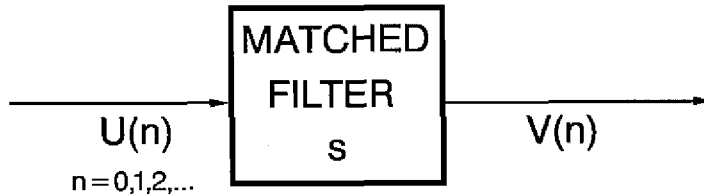


Fig. 7 — Sampled matched filter

Figure 7 shows the matched receiver structure. Here  $U(n)$  is the received time sampled input sequence consisting of signal plus noise. The received input sequence is convolved with conjugated time reversed vector of  $s$  which results in an output sequence  $V(n)$ . Mathematically, this is written

$$V(n) = \sum_{l=0}^{L-1} s_{l+1}^* U(n+l). \quad (7)$$

The sampled matched filter response of the desired signal vector  $s$  of length  $L$  is given by

$$r(m) = \begin{cases} \sum_{l=1}^{L-m} s_l s_{l+m}^*, & 0 \leq m \leq L-1, \\ \sum_{l=1}^{L+m} s_l^* s_{l-m}, & -(L-1) \leq m < 0. \end{cases} \quad (8)$$

This sequence is  $2L - 1$  points long and is often called the autocorrelation function (ACF) of  $s_1, s_2, \dots, s_{N-1}$ .

If we define

$$\mathbf{r} = (r(-(L-1)), \dots, r(-1), r(0), r(1), \dots, r(L-1))^T \quad (9)$$

and

$$S^T = \begin{bmatrix} s_L & 0 & 0 & \cdots & 0 \\ s_{L-1} & s_L & 0 & \cdots & 0 \\ s_{L-2} & s_{L-1} & s_L & \cdots & 0 \\ \vdots & \vdots & \vdots & \ddots & \vdots \\ \vdots & \vdots & \vdots & \cdots & \vdots \\ \vdots & \vdots & \vdots & \cdots & \vdots \\ s_1 & s_2 & s_3 & \cdots & s_L \\ 0 & s_1 & s_2 & \cdots & s_{L-1} \\ 0 & 0 & s_1 & \cdots & s_{L-2} \\ \vdots & \vdots & \vdots & \ddots & \vdots \\ \vdots & \vdots & \vdots & \cdots & \vdots \\ \vdots & \vdots & \vdots & \cdots & \vdots \\ 0 & 0 & 0 & \cdots & s_1 \end{bmatrix} \quad (10)$$

where  $\mathbf{r}$  is a  $2L - 1$  length vector, and  $S$  is a  $L \times (2L - 1)$  matrix called the ACF matrix of  $\mathbf{s}$ , we can show that

$$\mathbf{r} = S^t \mathbf{s} \quad (11)$$

where  $t$  is the conjugate transpose operation.

We assume for this analysis that the GS canceller processes data in blocks of  $K$  data samples per channel. Thus, the desired signal vector may be spread across a number of sample blocks. However, for this analysis, we assume the signal vector of length  $L$  is contained completely within the  $K$  data samples. Hence  $L \leq K$ . A future report will consider the effects of signal segmentation (i.e., when the signal is spread across a number of sample blocks of length  $K$ ). We define an augmented signal vector  $\mathbf{s}_{aug}$  of length  $K$  such that the first  $L$  elements are the elements of  $\mathbf{s}$  and the remaining elements are zero. Let  $\mathbf{s}'$  be the resultant output vector after  $\mathbf{s}$  has been processed through the GS canceller and  $\mathbf{s}'_{aug}$  be the resultant GS output augmented vector. This resultant output vector is then input into the matched filter of the vector  $\mathbf{s}$ , or equivalently  $\mathbf{s}_{aug}$ . If we set  $\mathbf{r}'$  equal to the response of  $\mathbf{s}'_{aug}$  match filtered with  $\mathbf{s}_{aug}$  then

$$\mathbf{r}' = S'_{aug} \mathbf{s}'_{aug} \quad (12)$$

where  $S_{aug}$  is defined as the  $K \times (2K - 1)$  augmented ACF matrix of  $\mathbf{s}_{aug}$ .

The results and derivations to be presented are the same whether we use the augmented or non-augmented notation. Hence, we assume that all vectors are augmented and drop the augmented designation. Note also that we have left-justified  $\mathbf{s}$  in  $\mathbf{s}_{aug}$ . Actually  $\mathbf{s}$  could start anywhere in  $\mathbf{s}_{aug}$ ; the assumption that the  $\mathbf{s}$  is left-justified is made for convenience's sake and does not change the results of this analysis.

Often  $\mathbf{s}$  is chosen so that the matched filter response has low sidelobes (i.e.,  $r(m) \ll r(0)$  for  $m \neq 0$ ). However, if the desired signal is passed through a GS canceller structure, the desired signal vector is perturbed and degradations occur in the matched filter response. Examples of codes that have high compression ratios and low sidelobes are the Frank Code [12], Lewis and Kretschmer's P1-P4 code [13], and shift register codes (also see Ref. 14). All of these codes have an ACF with all sidelobes well below the matched response. Figure 8 shows, for example, the ACF of the 100-element Frank code.

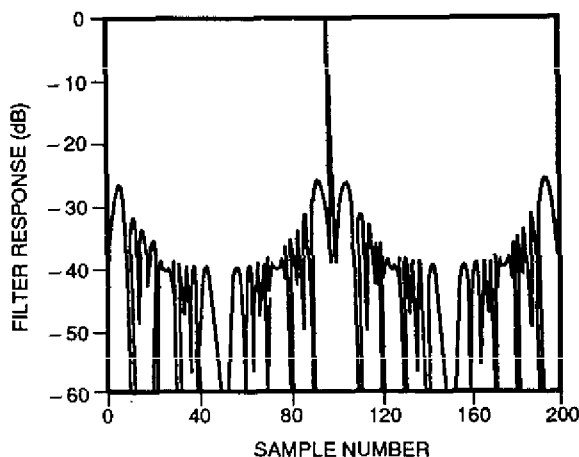


Fig. 8 — Frank code autocorrelation function  $L = 100$ , zero Doppler shift and no bandwidth limitation

#### 4. GS SIMPLIFICATIONS

This section discusses a number of results that significantly simplify the forthcoming analysis. Let  $C$  be any  $(N - 1) \times (N - 1)$  nonsingular matrix. It is well known [2] that transforming the auxiliary input channels  $x_1, \dots, x_{N-1}$  by this transform does not change the transient or steady-state noise power residue performance of the SMI (or GS). This is because the output from a canceller with transformed auxiliaries is identical to the output from a canceller with untransformed auxiliaries. The GS canceller implementation is equivalent to a matrix transforming the input channels. For a GS canceller, the matrix  $C$  has the upper triangular matrix form. In the configuration illustrated in Fig. 9 the matrix transform  $C$  is implemented by passing the input channels through a  $GS_{\infty, N}$  structure followed by a power equalizer on the output auxiliary channels. The output powers of the AUX channels after power equalization are equal to  $\sigma_{\min}^2$ . Without loss of generality, we can define  $\sigma_{\min}^2 = 1$ .

The structure shown in Fig. 9 illustrates that any GS canceller structure can be divided into two parts: a deterministic steady state front-end processor, in which the main channel is decorrelated from the auxiliary channels, and a stochastic back-end processor, which is driven by uncorrelated

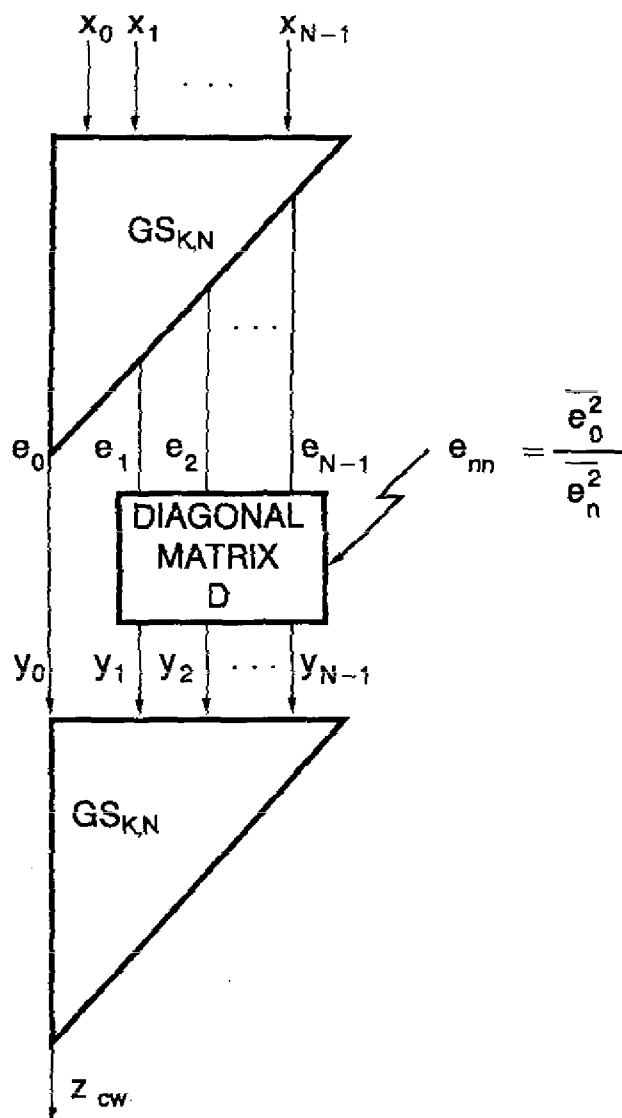


Fig. 9 — Residue equivalent  $GS_{K,N}$  canceller using the power equalizer matrix

equal powered noise in each channel. The back-end processor is independent of the input covariance matrix, and the auxiliary weights associated with the back end processor go to zero as  $K \rightarrow \infty$ . Hence, the convergence properties of the GS canceller can be studied by analyzing the convergence properties of the back-end processor. From this point on, we assume that the input channels are orthogonal and of equal power.

A second matrix transform that significantly simplifies the forthcoming analysis is now discussed. Let  $\Phi$  be any  $K \times K$  unitary matrix, i.e.  $\Phi' \Phi = I_K$ , where  $I_K$  is the  $K \times K$  identity matrix. Let us transform each input channel data set  $x_n$ ,  $n = 0, 1, 2, \dots, N - 1$  by  $\Phi$  such that

$$y_n = \Phi x_n, \quad n = 0, 1, \dots, N - 1, \quad (13)$$

where  $\mathbf{y}_n$ ,  $n = 0, 1, \dots, N - 1$  is the resultant output data set. If we input this data set into a  $\text{GS}_{K,N}$  canceller then [4] the estimated weights using the  $\mathbf{x}_n$  input are identical to those using the  $\mathbf{y}_n$  inputs.

Let

$$\mathbf{x}_n = (x_n(1), x_n(2), \dots, x_n(K))^T \quad (14)$$

be the  $K$ -length input vector in the  $n$ th channel and

$$\mathbf{z} = (z(1), z(2), \dots, z(K))^T \quad (15)$$

be the output vector of a  $\text{GS}_{K,N}$ . The  $\text{GS}_{K,N}$  canceller transforms the  $K$ -length data vectors  $\mathbf{x}_1, \mathbf{x}_2, \dots, \mathbf{x}_{N-1}$  into an orthogonal set of  $K$ -length data vectors  $\mathbf{z}_1, \mathbf{z}_2, \dots, \mathbf{z}_{N-1}$ . In fact, it was shown in Ref. 15 that

$$\mathbf{z} = G\mathbf{x}_0, \quad (16)$$

where  $G$  is the GS complementary projection matrix given by

$$G = I_K - \frac{\mathbf{z}_1 \mathbf{z}'_1}{\mathbf{z}'_1 \mathbf{z}_1} - \frac{\mathbf{z}_2 \mathbf{z}'_2}{\mathbf{z}'_2 \mathbf{z}_2} - \dots - \frac{\mathbf{z}_{N-1} \mathbf{z}'_{N-1}}{\mathbf{z}'_{N-1} \mathbf{z}_{N-1}}. \quad (17)$$

It was also shown that  $G$  can be written as

$$G = \Phi' \Lambda_{N-1} \Phi, \quad (18)$$

where  $\Phi$  is a  $K \times K$  unitary matrix that is a function of  $\mathbf{x}_n$ ,  $n = 1, 2, \dots, N-1$  and  $\Lambda_{N-1}$  is a  $K \times K$  diagonal matrix with the first  $N - 1$  diagonal elements equal to zero and the other diagonal elements equal to one. Thus

$$\mathbf{z} = \Phi' \Lambda_{N-1} \Phi \mathbf{x}_0. \quad (19)$$

We can write the  $K$ -length input vector in the main channel as

$$\mathbf{x}_M = \mathbf{s} + \mathbf{x}_0, \quad (20)$$

where  $\mathbf{s}$  denotes the  $K$ -length vector desired signal subcode and  $\mathbf{x}_0$  the  $K$ -length noise vector. Because of linearity, the  $\text{GS}_{K,N}$  canceller can be decomposed as shown in Fig. 10. Here the left hand  $\text{GS}_{K,N}$  canceller has only the desired signal in the main channel and the right-hand  $\text{GS}_{K,N}$  has only  $\mathbf{x}_0$  in the main channel. Note that the interior weights of the  $\text{GS}_{K,N}$  are not identical because of the different main channel in each (actually only the weights in the main channel differ). Hence, the left-hand  $\text{GS}_{K,N}$  output contains the perturbed desired signal output and the right-hand  $\text{GS}_{K,N}$  output contains the output noise residue. For the forthcoming analysis, we consider only the left hand output that contains the desired signal.

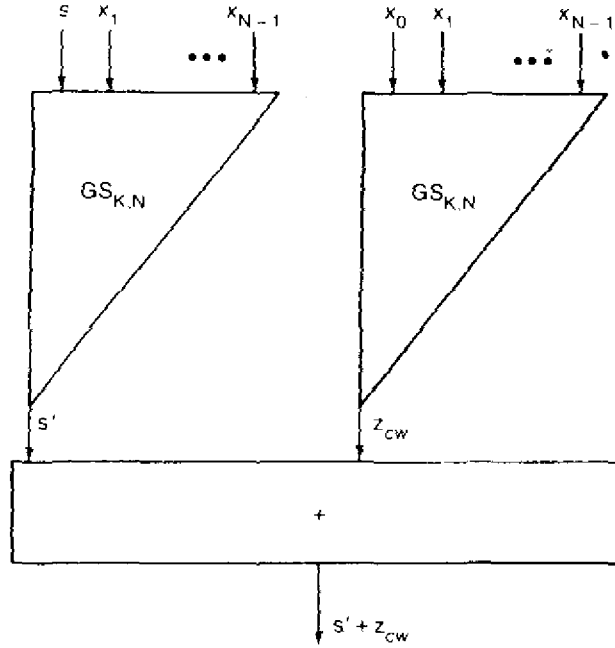


Fig. 10 — Decomposition of signal and noise for concurrent processing

Figure 9 shows that the desired signal passes unperturbed through the front-end processor  $GS_{\infty,N}$ . This is because the desired signal vector is a constant and, hence, is uncorrelated with the auxiliary channels. Thus the main channel weights in the  $GS_{\infty,N}$  canceller are zero. As a result, we need only consider the effects on the desired signal by the back-end processor where all the auxiliary channels are equipowered and independent random variables.

Finally, it was shown in Refs. 3 and 4 that if  $s_0$  and  $s_{N-1}$  are the input and output signal vectors respectively, of a  $GS_{K,N}$ , and the auxiliary inputs satisfy assumptions 1 through 5 (Section 2), then  $\eta = s'_{N-1}s_{N-1}/s'_0s_0$  has the following probability density function (PDF):

$$p(\eta) = \frac{(K-1)!}{(K-N)!(N-2)!} (1-\eta)^{N-2} \eta^{K-N}, \quad 0 \leq \eta \leq 1. \quad (21)$$

From this it is straightforward to show that for  $K \geq N$ ,

$$E\{s'_{N-1}s_{N-1}\} = \left[1 - \frac{N-1}{K}\right] s'_0s_0 \quad (22)$$

and

$$E\{|s'_{N-1}s_{N-1}|^2\} = \left[1 - \frac{2(N-1)}{K} + \frac{N(N-1)}{K(K+1)}\right] |s'_0s_0|^2 \quad (23)$$

and  $E\{\cdot\}$  denotes expectation.

## 5. SINGLE AUXILIARY CROSS-CORRELATIONS

This section presents derivations for two cross-correlations of outputs of a 2-input GS canceller. These expressions are fundamental in solving for the average pulse compression sidelobe increase when  $N > 2$ .

Consider two separate augmented signal vectors  $\mathbf{u}_0$  and  $\mathbf{v}_0$ . We assume that the desired signal vectors, each of length  $L$ , are completely contained in  $\mathbf{u}_0$  and  $\mathbf{v}_0$ , respectively. The augmented signal vectors have length  $K$ . Thus  $L \leq K$ . We input  $\mathbf{u}_0$  and  $\mathbf{v}_0$  into separate  $GS_{K,2}$  cancellers with a common auxiliary vector  $\mathbf{x}$  (Fig. 11). The  $K$  samples (or elements) of  $\mathbf{x}$  are random variables that satisfy assumptions 1 through 5 (Section 2).

The output signal vectors of the respective  $GS_{K,2}$  (Fig. 11) are denoted by  $\mathbf{u}_1$  and  $\mathbf{v}_1$ . We wish to find  $E\{|\mathbf{u}_1^t \mathbf{v}_1|^2\}$  and  $E\{\|\mathbf{u}_1\|^2 \|\mathbf{v}_1\|^2\}$  where for any vector  $\mathbf{c}$ ,  $\|\mathbf{c}\|^2 = \mathbf{c}^t \mathbf{c}$ .

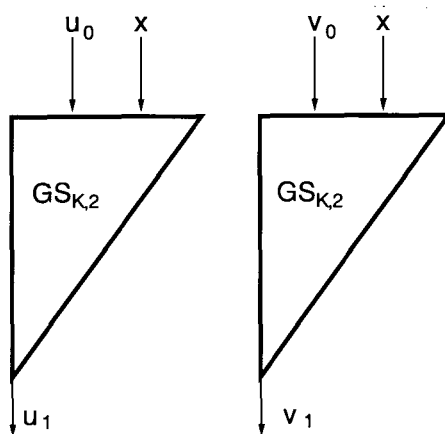


Fig. 11 — Parallel 2-input GS cancellers

From the previous section, we know that any  $K \times K$  unitary matrix transformation of each input vector into a GS canceller does not change the GS weights that are calculated thereafter. Furthermore, it is elementary to show that if  $\tilde{\mathbf{u}}_1$  and  $\tilde{\mathbf{v}}_1$  are the respective outputs of the unitary matrix transformed canceller, then

$$E\{|\mathbf{u}_1^t \mathbf{v}_1|^2\} = E\{|\tilde{\mathbf{u}}_1^t \tilde{\mathbf{v}}_1|^2\}, \quad (24)$$

and

$$E\{\|\mathbf{u}_1\|^2 \|\mathbf{v}_1\|^2\} = E\{\|\tilde{\mathbf{u}}_1\|^2 \|\tilde{\mathbf{v}}_1\|^2\}. \quad (25)$$

We use this relationship to simplify the input signal vectors  $\mathbf{u}_0$  and  $\mathbf{v}_0$ . It can be shown [16] that a  $K \times K$  unitary matrix  $\Phi$  exists, such that

$$\tilde{\mathbf{u}}_0 = \Phi \mathbf{u}_0 = \|\mathbf{u}_0\|(1, 0, 0, \dots, 0)^T, \quad (26)$$

and

$$\tilde{\mathbf{v}}_0 = \Phi \mathbf{v}_0 = \|\mathbf{v}_0\|(\rho, \sqrt{1 - |\rho|^2}, 0, 0, \dots, 0)^T, \quad (27)$$

where

$$\rho = \frac{\mathbf{u}_0^t \mathbf{v}_0}{\|\mathbf{u}_0\| \|\mathbf{v}_0\|}, \quad (28)$$

and we have defined  $\tilde{\mathbf{u}}_0$  and  $\tilde{\mathbf{v}}_0$  as the unitary matrix transformed input vectors. Set

$$\mathbf{y} = \Phi \mathbf{x}. \quad (29)$$

Note that because  $\mathbf{x}$  is a normalized  $K$ -length multivariate complex circular Gaussian vector,  $\mathbf{y} = (y_1, y_2, \dots, y_K)^T$  is also.

The  $K$ -length output vectors of each  $GS_{K,2}$  are given by

$$\tilde{\mathbf{u}}_1 = \tilde{\mathbf{u}}_0 - \frac{\mathbf{y}' \tilde{\mathbf{u}}_0}{\mathbf{y}' \mathbf{y}} \mathbf{y} = \left( I_K - \frac{\mathbf{y} \mathbf{y}'}{\mathbf{y}' \mathbf{y}} \right) \tilde{\mathbf{u}}_0 \quad (30)$$

and

$$\tilde{\mathbf{v}}_1 = \tilde{\mathbf{v}}_0 - \frac{\mathbf{y}' \tilde{\mathbf{v}}_0}{\mathbf{y}' \mathbf{y}} \mathbf{y} = \left( I_K - \frac{\mathbf{y} \mathbf{y}'}{\mathbf{y}' \mathbf{y}} \right) \tilde{\mathbf{v}}_0, \quad (31)$$

where  $I_K$  is the  $K \times K$  identity matrix. We can show that

$$\tilde{\mathbf{u}}_1^t \tilde{\mathbf{v}}_1 = \|\mathbf{u}_0\| \|\mathbf{v}_0\| \left[ \rho \left( 1 - \frac{|y_1|^2}{\mathbf{y}' \mathbf{y}} \right) - \sqrt{1 - |\rho|^2} \frac{y_1 y_2^*}{\mathbf{y}' \mathbf{y}} \right], \quad (32)$$

$$\|\tilde{\mathbf{u}}_1\|^2 = \|\mathbf{u}_0\|^2 \left[ 1 - \frac{|y_1|^2}{\mathbf{y}' \mathbf{y}} \right], \quad (33)$$

and

$$\|\tilde{\mathbf{v}}_1\|^2 = \|\mathbf{v}_0\|^2 \left[ 1 - \frac{|\rho^* y_1 + \sqrt{1 - |\rho|^2} y_2|^2}{\mathbf{y}' \mathbf{y}} \right]. \quad (34)$$

It is shown in the Appendix that

$$E\{|\mathbf{u}_1^t \mathbf{v}_1|^2\} = E\{|\tilde{\mathbf{u}}_1^t \tilde{\mathbf{v}}_1|^2\} = |\mathbf{u}_0^t \mathbf{v}_0|^2 \left[ 1 - \frac{2}{K} + \frac{1}{K(K+1)} \right] + \frac{\|\mathbf{u}_0\|^2 \|\mathbf{v}_0\|^2}{K(K+1)} \quad (35)$$

and

$$E\{\|\mathbf{u}_1\|^2 \|\mathbf{v}_1\|^2\} = E\{\|\tilde{\mathbf{u}}_1\|^2 \|\tilde{\mathbf{v}}_1\|^2\} = \frac{|\mathbf{u}_0^t \mathbf{v}_0|^2}{K(K+1)} + \|\mathbf{u}_0\|^2 \|\mathbf{v}_0\|^2 \left[ 1 - \frac{2}{K} + \frac{1}{K(K+1)} \right]. \quad (36)$$

## 6. MULTIPLE AUXILIARY CROSS-CORRELATIONS

In this section, we derive expressions for two cross-correlations of outputs of an  $N$ -input GS canceller. The input signal vectors  $\mathbf{u}_0$  and  $\mathbf{v}_0$  are as defined in the previous section. We input  $\mathbf{u}_0$  and  $\mathbf{v}_0$  to separate  $GS_{K,N}$  cancellers with common auxiliary vectors  $\mathbf{x}_1, \mathbf{x}_2, \dots, \mathbf{x}_{N-1}$  as illustrated in Fig. 12. The  $K$  samples (or elements) of each auxiliary vector  $\mathbf{x}_1, \dots, \mathbf{x}_{N-1}$ , are r.v.s that satisfy assumptions 1 through 5 (Section 2). Let the signal output at each level of the respective  $GS_{K,N}$  be denoted by  $\mathbf{u}_n$  and  $\mathbf{v}_n$ ,  $n = 0, 1, \dots, N - 1$ . We wish to find  $E\{|\mathbf{u}_{N-1}'\mathbf{v}_{N-1}|^2\}$  and  $E\{\|\mathbf{u}_{N-1}\|^2\|\mathbf{v}_{N-1}\|^2\}$ . It will be found that this can be done recursively.

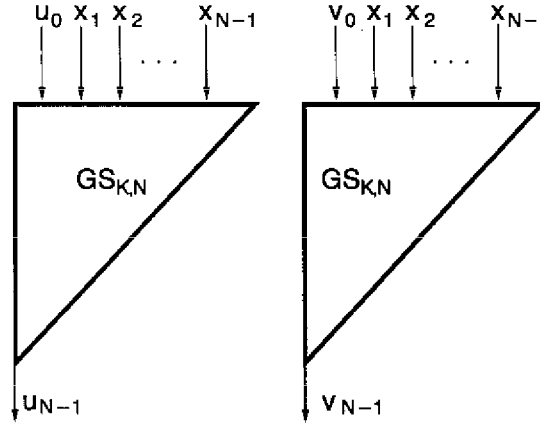


Fig. 12 — Parallel  $N$ -input GS cancellers

To this end, as in the previous section, we multiply  $\mathbf{u}_0$  and  $\mathbf{v}_0$  by a unitary matrix transformation  $\Phi$ , such that the new input vectors  $\tilde{\mathbf{u}}_0$  and  $\tilde{\mathbf{v}}_0$  are given by Eqs. (26) and (27). It is straightforward to show that

$$E\{|\mathbf{u}_n'\mathbf{v}_n|^2\} = E\{|\tilde{\mathbf{u}}_n'\tilde{\mathbf{v}}_n|^2\}, \quad E\{\|\mathbf{u}_n\|^2\|\mathbf{v}_n\|^2\} = E\{\|\tilde{\mathbf{u}}_n\|^2\|\tilde{\mathbf{v}}_n\|^2\} \quad (37)$$

for  $n = 0, 1, \dots, N - 1$ . In addition, each of the auxiliary input data vectors is multiplied by  $\Phi$  such that  $\tilde{\mathbf{x}}_n = \Phi\mathbf{x}_n$ ,  $n = 1, 2, \dots, N - 1$ . Note that each of the transformed auxiliary vectors also satisfies assumptions 1 through 5 and is statistically identical to  $\mathbf{x}_n$ ,  $n = 1, 2, \dots, N - 1$ .

We redraw the configurations seen in Fig. 12 into the equivalent configurations seen in Fig. 13. Here we show for each of the original  $GS_{K,N}$  cancellers decomposed into two  $GS_{K,N-1}$  parallel cancellers followed by a single  $GS_{K,2}$  canceller. The  $K$ -length noise vector into the  $GS_{K,2}$  cancellers is denoted by  $\mathbf{y}$ .

As stated in Section 4, we can write

$$\tilde{\mathbf{u}}_{N-2} = \Phi_0' \Lambda_{N-2} \Phi_0 \tilde{\mathbf{u}}_0, \quad (38)$$

$$\tilde{\mathbf{v}}_{N-2} = \Phi_0' \Lambda_{N-2} \Phi_0 \tilde{\mathbf{v}}_0, \quad (39)$$

and

$$\mathbf{y} = \Phi_0' \Lambda_{N-2} \Phi_0 \mathbf{x}_1, \quad (40)$$

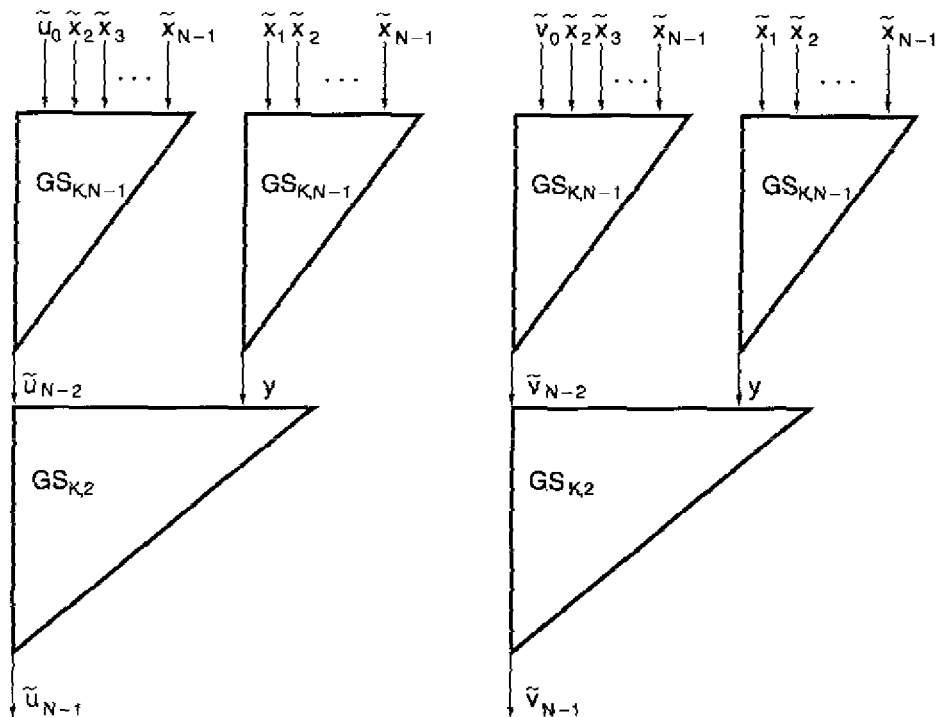


Fig. 13 — Equivalent representation of Fig. 12

where  $\Phi_0$  is a  $K \times K$  unitary matrix that is a function of  $x_2, x_3, \dots, x_{N-1}$  and  $\Lambda_{N-2}$  is a  $K \times K$  diagonal matrix with the first  $N-2$  diagonal elements equal to zero. All other diagonal elements are equal to one.

If we premultiply  $\tilde{u}_{N-2}$ ,  $\tilde{v}_{N-2}$ , and  $y$  by the unitary matrix  $\Phi_0$ , the resultants of the cross-correlations we are seeking do not change. However, the number of independent and identically distributed (i.i.d.) elements in the auxiliary vector is reduced by  $N-2$  as indicated by Eq. (40). The first  $N-2$  elements of  $\Phi y$ ,  $\Phi \tilde{u}_{N-1}$ , and  $\Phi \tilde{v}_{N-2}$  are zero. Hence, it follows using the methodology given in the previous section for finding cross-correlations for an arbitrary number of i.i.d. samples in the auxiliary channel of a 2-input GS that the expectations of these cross-correlations conditioned on  $x_2, \dots, x_{N-1}$  are given by

$$E\{|\tilde{u}'_{N-1}\tilde{v}_{N-1}|^2 | x_2, \dots, x_{N-1}\} \quad (41)$$

$$= |\tilde{u}'_{N-2}\tilde{v}_{N-2}|^2 \left[ 1 - \frac{2}{K-N+2} + \frac{1}{(K-N+2)(K-N+3)} \right] + \frac{\|\tilde{u}_{N-2}\|^2 \|\tilde{v}_{N-2}\|^2}{(K-N+2)(K-N+3)},$$

and

$$E\{\|\tilde{u}_{N-1}\|^2 \|\tilde{v}_{N-1}\|^2 | x_2, \dots, x_{N-1}\} \quad (42)$$

$$= \frac{|\tilde{u}'_{N-2}\tilde{v}_{N-2}|^2}{(K-N+2)(K-N+2)} + \|\tilde{u}_{N-2}\|^2 \|\tilde{v}_{N-2}\|^2 \left[ 1 - \frac{2}{(K-N+2)} + \frac{1}{(K-N+2)(K-N+3)} \right].$$

By integrating over the conditional r.v.s, we find

$$\begin{aligned}
 & E\{|\mathbf{u}'_{N-1}\mathbf{v}_{N-1}|^2\} \\
 &= E\{|\mathbf{u}'_{N-2}\mathbf{v}_{N-2}|^2\} \left[ 1 - \frac{2}{K-N+2} + \frac{1}{(K-N+2)(K-N+3)} \right] \\
 &\quad + E\{\|\mathbf{u}_{N-2}\|^2\|\mathbf{v}_{N-2}\|^2\} \frac{1}{(K-N+2)(K-N+3)} \\
 E\{\|\mathbf{u}_{N-1}\|^2\|\mathbf{v}_{N-1}\|^2\} &= E\{|\mathbf{u}'_{N-2}\mathbf{v}_{N-2}|^2\} \frac{1}{(K-N+2)(K-N+3)} \\
 &\quad + E\{\|\mathbf{u}_{N-2}\|^2\|\mathbf{v}_{N-2}\|^2\} \left[ 1 - \frac{2}{K-N+2} + \frac{1}{(K-N+2)(K-N+3)} \right], \quad (43)
 \end{aligned}$$

where we have dropped the tilde over the output variables in lieu of Eq. (37).

It is apparent that the desired moments can be found through recursion. Set

$$\alpha_n = E\{|\mathbf{u}'_n\mathbf{v}_n|^2\}, \quad (44)$$

$$\beta_n = E\{\|\mathbf{u}_n\|^2\|\mathbf{v}_n\|^2\}, \quad (45)$$

$$a_n = 1 - \frac{2}{K-n} + \frac{1}{(K-n)(K-n+1)}, \quad (46)$$

and

$$b_n = \frac{1}{(K-n)(K-n+1)}. \quad (47)$$

It then follows that the recursion equations are

$$\alpha_{n+1} = a_n\alpha_n + b_n\beta_n \quad (48)$$

and

$$\beta_{n+1} = b_n\alpha_n + a_n\beta_n, \quad (49)$$

with initial conditions (I.C.)

$$\alpha_0 = |\mathbf{u}'_0\mathbf{v}_0|^2, \quad \beta_0 = \|\mathbf{u}_0\|^2\|\mathbf{v}_0\|^2. \quad (50)$$

We rewrite Eqs. (48-50) in vector form by defining  $\epsilon_n = (\alpha_n, \beta_n)^T$  as

$$\epsilon_{n+1} = \begin{bmatrix} a_n & b_n \\ b_n & a_n \end{bmatrix} \epsilon_n, \quad \text{I.C.: } \epsilon_0 = \begin{bmatrix} |\mathbf{u}_0^T \mathbf{v}_0|^2 \\ \|\mathbf{u}_0\|^2 \|\mathbf{v}_0\|^2 \end{bmatrix}. \quad (51)$$

Thus solving for  $\epsilon_{N-1}$ :

$$\epsilon_{N-1} = \begin{bmatrix} N-2 \\ \prod_{n=0} \end{bmatrix} \begin{bmatrix} a_n & b_n \\ b_n & a_n \end{bmatrix} \begin{bmatrix} |\mathbf{u}_0^T \mathbf{v}_0|^2 \\ \|\mathbf{u}_0\|^2 \|\mathbf{v}_0\|^2 \end{bmatrix}. \quad (52)$$

The desired cross correlations are given by the elements of  $\epsilon_{N-1}$  where  $E\{|\mathbf{u}_{N-1}^T \mathbf{v}_{N-1}|^2\}$  and  $E\{\|\mathbf{u}_{N-1}\|^2 \|\mathbf{v}_{N-1}\|^2\}$  are given by the first and second elements, respectively.

Define

$$A = \begin{bmatrix} A_{11}(K, N) & A_{12}(K, N) \\ A_{21}(K, N) & A_{22}(K, N) \end{bmatrix} = \prod_{n=0}^{N-2} \begin{bmatrix} a_n & b_n \\ b_n & a_n \end{bmatrix}. \quad (53)$$

Then

$$E\{|\mathbf{u}_{N-1}^T \mathbf{v}_{N-1}|^2\} = A_{11}(K, N) |\mathbf{u}_0^T \mathbf{v}_0|^2 + A_{12}(K, N) \|\mathbf{u}_0\|^2 \|\mathbf{v}_0\|^2 \quad (54)$$

and

$$E\{\|\mathbf{u}_{N-1}\|^2 \|\mathbf{v}_{N-1}\|^2\} = A_{21}(K, N) |\mathbf{u}_0^T \mathbf{v}_0|^2 + A_{22}(K, N) \|\mathbf{u}_0\|^2 \|\mathbf{v}_0\|^2. \quad (55)$$

We note that because of the symmetries in form of the  $2 \times 2$  matrix  $A$  defined in Eq. (53), we can show that  $A_{21}(K, N) = A_{12}(K, N)$ . In fact, if we evaluate Eqs. (54) and (55) at  $\mathbf{u}_0 = \mathbf{v}_0$ , we find that

$$A_{11}(K, N) = A_{22}(K, N) \quad (56)$$

and using Eq. (23)

$$A_{11}(K, N) + A_{12}(K, N) = 1 - \frac{2(N-1)}{K} + \frac{N(N-1)}{K(K+1)}. \quad (57)$$

## 7. SIDELobe DEGRADATION DERIVATION

We now derive an exact expression for the average adaptive pulse compressed sidelobe by using the result of the previous section. The desired input signal vector is assumed not to be segmented (i.e., it is contained entirely in the augmented signal vector denoted by  $\mathbf{s}_0$ ). Each auxiliary channel has  $K$  samples and these samples satisfy assumptions 1 through 5. Also, the desired signal vector is normalized so that  $\|\mathbf{s}_0\|^2 = 1$

Figure 14 shows the  $N$ -input canceller followed by the matched filter. Let  $s_c$  be defined as any column of the augmented ACF matrix. Then, an expression representing an output  $r$  of the matched filter (match point or sidelobes) after cancellation is given by

$$r = s_c^t s_{N-1} \quad (58)$$

where  $s_{N-1}$  is the  $K$ -length output signal vector of the  $GS_{K,N}$  canceller.

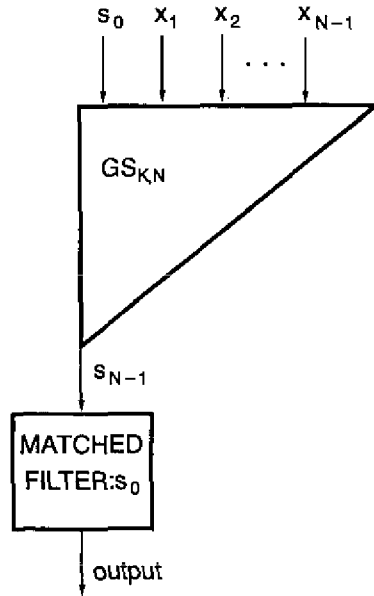


Fig. 14 — GS canceller followed by a matched filter

We define the average adaptive pulse compression sidelobe level associated with  $s_c$  as  $SL_{a,c}$ , which is given by

$$SL_{a,c} = \frac{E\{|s_c^t s_{N-1}|^2\}}{E\{|s_{N-1}^t s_{N-1}|^2\}} \quad (59)$$

As  $K \rightarrow \infty$ , note that  $s_{N-1} \rightarrow s_0$  and  $SL_{a,c}$  goes to the quiescent sidelobe level of  $s_c$ . This equals  $|s_c^t s_0|^2$  which is given as  $SL_{q,c}$ . We normalized by the adaptive match point response  $E\{|s_{N-1}^t s_{N-1}|^2\}$ , just as  $|s_c^t s_0|^2$  would be normalized with the quiescent match point response  $|s_0^t s_0|^2$ .

The denominator of Eq. (59) was evaluated in Refs. 3 and 4 and in Section 4 and is given by

$$\begin{aligned} E\{|s_{N-1}^t s_{N-1}|^2\} &= 1 - \frac{2(N-1)}{K} + \frac{N(N-1)}{K(K+1)} \\ &= \frac{(K-N+1)(K-N+2)}{K(K+1)}. \end{aligned} \quad (60)$$

The numerator of Eq. (59) is evaluated by using the results of the previous sections. As stated in Section 4, if  $\mathbf{s}_0$  and  $\mathbf{s}_c$  are the main channel inputs to two distinct  $GS_{K,N}$  cancellers with identical auxiliary inputs, then the outputs of these two cancellers can be written as

$$\mathbf{s}_{N-1} = \Phi^t \Lambda_{N-1} \Phi \mathbf{s}_0, \quad (61)$$

$$\mathbf{s}_{c,N-1} = \Phi^t \Lambda_{N-1} \Phi \mathbf{s}_c, \quad (62)$$

where  $\Phi$  is a  $K \times K$  unitary matrix. Using Eqs. (61) and (62), it can be shown that

$$\mathbf{s}_{c,N-1}^t \mathbf{s}_{N-1} = \mathbf{s}_c^t \mathbf{s}_0. \quad (63)$$

Thus

$$E\{|\mathbf{s}_c^t \mathbf{s}_{N-1}|^2\} = E\{|\mathbf{s}_{c,N-1}^t \mathbf{s}_{N-1}|^2\}, \quad (64)$$

and the analysis of Section 6 can be applied with  $\mathbf{u}_0 = \mathbf{s}_c$  and  $\mathbf{v}_0 = \mathbf{s}_0$ .

Using Eq. (54) and the fact that  $\|\mathbf{s}_0\|^2 = 1$ , it follows that

$$E\{|\mathbf{s}_{c,N-1}^t \mathbf{s}_{N-1}|^2\} = A_{11}(K, N) |\mathbf{s}_c^t \mathbf{s}_0|^2 + A_{12}(K, N) \|\mathbf{s}_c\|^2. \quad (65)$$

Substituting Eq. (60) and (65) into Eq. (59) results in

$$SL_{a,c} = \frac{K(K+1) A_{11}(K, N)}{(K-N+1)(K-N+2)} SL_{q,c} + \frac{K(K+1) A_{12}(K, N)}{(K-N+1)(K-N+2)} \|\mathbf{s}_c\|^2. \quad (66)$$

We define

$$Q(K, N) = \frac{K(K+1) A_{11}(K, N)}{(K-N+1)(K-N+2)} \quad (67)$$

to be the quiescent sidelobe factor and

$$\Delta SL_a(K, N) = \frac{K(K+1) A_{12}(K, N)}{(K-N+1)(K-N+2)} \quad (68)$$

to be the adaptive sidelobe perturbation. Note  $\Delta SL_a(K, N)$  is constant over all sidelobes of the compressed pulse.

## 8. RESULTS

For the results to be presented, it is convenient to set  $N_{aux} = N - 1$  where  $N_{aux}$  is the number of auxiliary channels. In addition, the number of independent samples per channel  $K$  is set equal to

an integer multiple of  $N_{aux}$ . Let  $K = MN_{aux}$  and  $Q_0(M, N_{aux}) = Q(K, N)$  where  $Q(K, N)$  is defined by Eq. (68). To achieve good signal detection and noise cancellation, for most practical cases  $M \geq 2$ , [2-5,17]. Figure 15 presents the quiescent sidelobe factor  $Q_0(M, N_{aux})$  plotted in dB vs  $N_{aux}$  and  $M$ . Note for all  $M \geq 2$  and  $N_{aux}$  that  $Q_0(M, N_{aux})$  is less than and approximately equal to one. Hence the approximation that  $Q_0(M, N) = 1$  is valid in most cases. Reexamining Eq. (67) indicates that for  $M \geq 2$ , the adaptive sidelobe level is equal to the quiescent sidelobe level plus the adaptive sidelobe perturbation term given by Eq. (69) which we denote as  $\Delta SL_a(K, N) \|s_c\|^2$ .

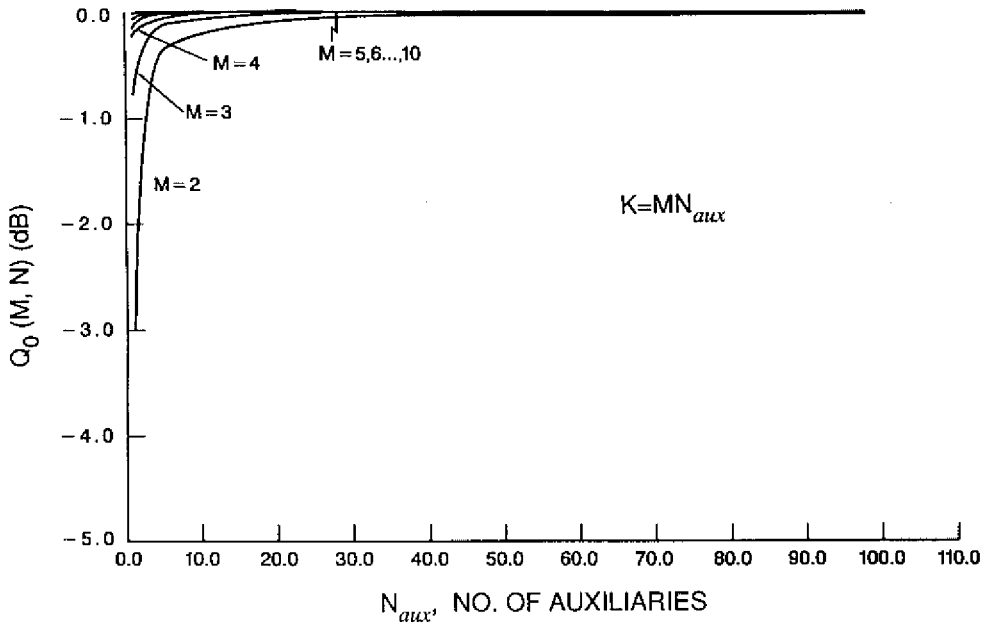


Fig. 15 — Quiescent sidelobe factor vs  $N_{aux}$  and  $N$

Assume  $\max \|s_c\|^2 \approx 1$ . Figure 16 plots  $\max \Delta SL_a$  vs  $N_{aux}$  and  $M$ . These curves establish a performance floor for the peak adaptive pulse compression sidelobes. For a given  $N_{aux}$  and  $K$  (or  $MN_{aux}$ ), the adaptive compressed sidelobe level on the average is greater than the  $\Delta SL_a$  calculated for  $N_{aux}$  and  $K$ . This figure shows that  $\max \Delta SL_a$  decreases monotonically with  $M$  and  $N_{aux}$ . Hence, two ways of decreasing the performance floor are to increase either the number of independent input samples or the number of auxiliary channels. We also observe that more than 5  $N_{aux}$  independent samples are necessary to achieve a modest adaptive compressed sidelobe level of  $-25$  dB for fewer than 20 auxiliaries.

It is significant to note that even had the waveform been pulse-compressed into a single range bin before the cancellation process, the maximum range sidelobe level after cancellation would be the same as if the waveform had been compressed after the canceller. To see this, assume  $s = (1, 0, 0, \dots, 0)^T$ . This input vector corresponds to the output of a perfect pulse compressor; i.e., all of the signal energy is in one range cell (we are assuming a sampling rate equal to the waveform bandwidth). If this waveform is input to the canceller, processed, and matched filtered with  $s = (1, 0, \dots, 0)^T$ , then Eq. (67) indicates that this input signal vector has maximum range sidelobe levels equal to  $\Delta SL_a(K, N)$ . Hence, the same perturbed sidelobe level results regardless of whether

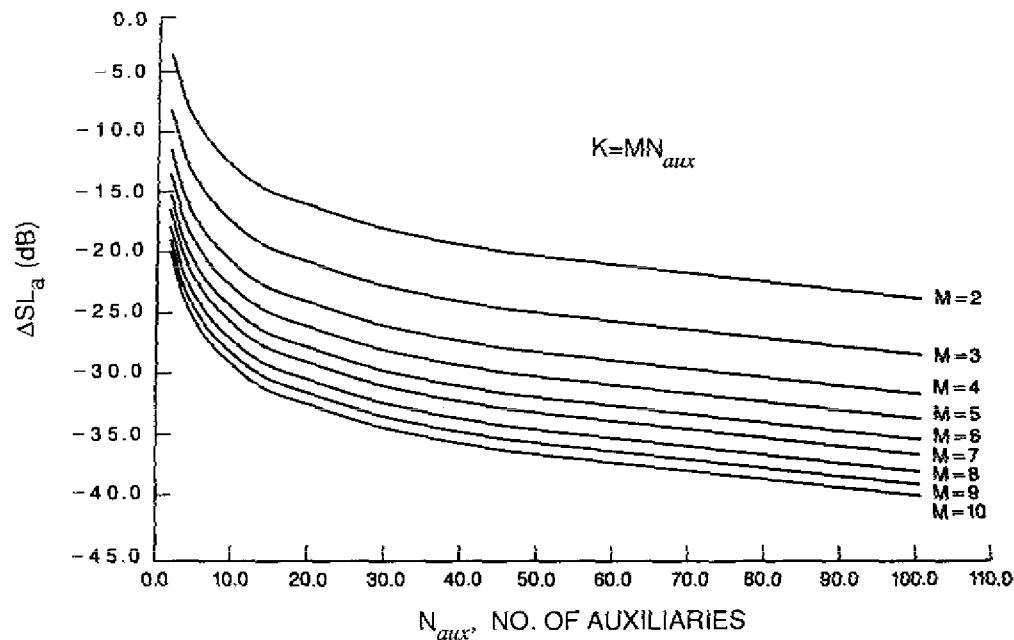


Fig. 16 — Maximum adaptive sidelobe perturbations vs  $N_{aux}$  and  $M$ ; signal completely contained in  $K$  input samples

pulse compression occurs before or after cancellation. Again, note that we are assuming the uncompressed pulse is completely contained in the  $K$  samples used to calculate the canceller weights. Thus, it would seem desirable if  $L \ll K$  to place the pulse compression after the canceller because of the previously cited disadvantages (see Section 1) of having it before the canceller. If the uncompressed waveform extends over a number of batches of  $K$  samples, it might be more desirable to do pulse compression first to prevent the compressed pulse's canceller-induced higher sidelobes from extending over these batches. A future study will address this issue.

The above analysis of pulse compression and canceller interactions can also be applied to quantifying the canceller degradation caused by the presence of a desired signal in the samples used to calculate the adaptive canceller weights. If the desired signal has the power  $\sigma_s^2$  after pulse compression, then the average power residue from the signal in the  $K - 1$  range bins not containing the signal can be shown from our analysis to equal at most  $\sigma_s^2 \Delta SL_a(K, N)$  plus possibly the signal power resulting from the quiescent compressed sidelobes. Now  $\sigma_s^2 \Delta SL_a(K, N)$  might be much greater than the quiescent output noise power level  $\sigma_{min}^2$  of the canceller. However,  $\Delta SL_a(K, N)$  is a function of  $N$  and  $K$ , and with increasing  $K$  can be made as small as desired. Hence, by using the values of  $\sigma_s^2$ ,  $N$ , and  $\sigma_{min}^2$  in conjunction with Fig. 16, one can find the number of independent samples  $K$  needed such that  $\sigma_s^2 \Delta SL_a(K, N)$  is within 3 dB of  $\sigma_{min}^2$ .

We note that in some canceller schemes the adaptive weights are computed from the  $K/2$  samples before and after a chosen sample. Hence the chosen sample itself is not used in the weight evaluation. This technique's advantage is that if the desired signal is localized to a single range sample the undesirable effect of cancelling the desired signal does not occur [3,4]. However, a noise power residue from the desired signal is present in the canceller output samples preceding and following the chosen sample because the signal is present in the weight calculation for these samples. This

level occurs in the  $K/2$  samples before and after the chosen sample. The maximum level of the signal-induced canceller residue is equal to  $\sigma_s^2 \Delta SL_q(K, N)$ . Again,  $K$  can be chosen large enough to be within 3 dB of  $\sigma_{\min}^2$ .

One final note: for some applications, the matched filter is replaced by a filtering scheme whereby the range sidelobes are reduced at the expense of signal gain at the match point. However, the results derived in this report are also valid if any filter other than the matched filter  $s_0$  is used. We could replace the  $s_0$  seen in the "matched filter" block in Fig. 14 with a general weighting function given by the  $L$ -length vector,  $\mathbf{a}$  with elements  $a_0, a_1, \dots, a_{L-1}$ . In our analysis, we would replace the  $S$  matrix defined by Eq. (10) with an  $A$  matrix whose elements are given by replacing the  $s$  s with  $a$  s in Eq. (10). The vector  $s_c$  then would be taken to be any column in  $A$  and the analysis follows as given.

## 9. SUMMARY

Performance results for the sidelobe level of a compressed pulse that has been preprocessed through an adaptive canceller have been obtained. The adaptive canceller is implemented by using the Sampled Matrix Inversion (SMI) algorithm. Because of finite sampling, the quiescent compressed pulse sidelobe levels are degraded because of the preprocessing of the main channel input data stream (i.e., the uncompressed pulse) through an adaptive canceller. An exact expression was derived for the average adaptive pulse compression sidelobe level that was found to be a function of the number of auxiliary input canceller channels  $N_{aux}$ , the number of independent samples per channel  $K$ , and the given input code of length  $L$ . It was shown that  $K/N_{aux}$  can be significantly greater than one to retain sidelobes that are close to the original quiescent sidelobe level (with no adaptive canceller). Also, it was shown that the maximum sidelobe level degradation is independent of whether pulse compression occurs before or after the adaptive canceller if the uncompressed pulse is completely contained within the  $K$  samples that are used to calculate the canceller weights. It was further shown that this same analysis can be used to predict the noise power level at the canceller output, that is induced by having the desired signal present in the canceller weight calculation.

## REFERENCES

1. R.A. Monzingo and T.W. Miller, *Introduction to Adaptive Arrays* (John Wiley & Sons, New York, 1980) Ch. 8.
2. I.S. Reed, J.D. Mallett, and L.E. Brennan, "Rapid Convergence Rate in Adaptive Arrays," *IEEE Trans. Aerospace Electron. Sys.* **AES-10**, 853-863 (1974).
3. L.E. Brennan and I.S. Reed, "Digital Adaptive Arrays with Weights Computed from and Applied to the Same Sample Set," Proceedings of the 1980 Adaptive Antenna Symposium, RADC-TR-80-378, Vol. 1, Dec. 1980.
4. Karl Gerlach and F.F. Kretschmer, Jr., "Convergence Properties of the Gram-Schmidt and SMI Adaptive Algorithms," *IEEE Trans. Aerospace Electron. Sys.* **AES-26**, 44-57 (1991).
5. Karl Gerlach, "Sidelobe Level of an Adaptive Array Using the SMI Algorithm," NRL Report 9079, Feb. 1988.

KARL GERLACH

6. B.L. Lewis and F.F. Kretschmer, Jr., published work of limited distribution, Feb. 1974.
7. M.A. Alam, "Orthonormal Lattice Filter—A Multistage, Multichannel Estimation Technique," *Geophys.* **43**, 1368-1382 (1978).
8. Karl Gerlach, "Fast Orthogonalization Networks," *IEEE Trans. Antennas Propag.* **AP-34**(3), 458-462 (1986).
9. D.O. North, "Analysis of the Factors which Determine Signal/Noise Discrimination in Radar," *Proc. IEEE* **51**, 1016-1027 (1963).
10. H.L. van Trees, *Detection, Estimation, and Modulation Theory, Part I* (John Wiley & Sons Inc., New York, 1968) Ch. 3.
11. M.I. Skolnik, *Introduction to Radar Systems* (McGraw-Hill, New York, 1980).
12. R.L. Frank, "Polyphase Codes with Good Nonperiodic Correlation Properties," *IEEE Trans. Inf. Theory* **IT-9**, 43-45 (1963).
13. B.L. Lewis, F.F. Kretschmer, Jr., and W.W. Shelton, *Aspects of Radar Signal Processing* (Artech House Inc., Norwood, MA, 1986) Ch. 2.
14. F.F. Kretschmer, Jr. and Karl Gerlach, "Radar Waveforms Derived from Orthogonal Matrices," NRL Report 9080, Feb. 1989.
15. Karl Gerlach and F.F. Kretschmer, Jr., "Convergence Properties of the Gram-Schmidt and SMI Adaptive Algorithms, Part 2," *IEEE Trans. Aerospace Electron. Sys.* **AES-27**, 83-91 (1991).
16. C.M. Rader and A.O. Steinhardt, "Hyperbolic Householder Transformations," *IEEE Trans. Acoustics, Speech, Signal Proc.* **ASSP-35**(6), 1589-1602 (1966).
17. E.J. Kelly, "An Adaptive Detection Algorithm," *IEEE Trans. Aerospace Electron. Sys.* **AES-22**(1), 115-127 (1986).

**Appendix**  
**DERIVATION OF EQS. (35)-(36)**

Starting with Eq. (32), we first derive Eq. (35). Now

$$E\{|\tilde{\mathbf{u}}_1' \tilde{\mathbf{v}}_1|^2\} = \|\tilde{\mathbf{u}}_0\|^2 \|\tilde{\mathbf{v}}_0\|^2 \left[ |\rho|^2 E\left\{\left[1 - \frac{|y_1|^2}{\mathbf{y}'\mathbf{y}}\right]^2\right\} + (1 - |\rho|^2) E\left\{\frac{|y_1|^2 |y_2|^2}{(\mathbf{y}'\mathbf{y})^2}\right\} \right]. \quad (\text{A1})$$

Note that the expected values of the cross-terms resulting from magnitude-squaring the right side of Eq. (32) are zero because  $y_2$  is zero mean. Now for  $\rho = 1$ , we can show using Eqs. (A1) and (23) that

$$E\left\{\left[1 - \frac{|y_1|^2}{\mathbf{y}'\mathbf{y}}\right]^2\right\} = 1 - \frac{2}{K} + \frac{2}{K(K+1)}. \quad (\text{A2})$$

From Eq. (A2), it can be shown that

$$E\left\{\frac{|y_1|^4}{(\mathbf{y}'\mathbf{y})^2}\right\} = \frac{2}{K(K+1)}. \quad (\text{A3})$$

Now

$$E\left\{\frac{(\mathbf{y}'\mathbf{y})^2}{(\mathbf{y}'\mathbf{y})^2}\right\} = 1 = \sum_{k=1}^K E\left\{\frac{|y_k|^4}{(\mathbf{y}'\mathbf{y})^2}\right\} + \sum_{\substack{k_1=1 \\ k_1 \neq k_2}}^K \sum_{k_2=1}^K E\left\{\frac{|y_{k_1}|^2 |y_{k_2}|^2}{(\mathbf{y}'\mathbf{y})^2}\right\}. \quad (\text{A4})$$

Because  $y_1, y_2, \dots, y_K$  are identically distributed r.v.s, the terms in the first summation are all equal and the terms in the double summation are equal. Let

$$a = E\left\{\frac{|y_1|^2 |y_2|^2}{(\mathbf{y}'\mathbf{y})^2}\right\}. \quad (\text{A5})$$

Substituting Eqs. (A3) and (A5) into Eq. (A4) results in

$$K \cdot \frac{2}{K(K+1)} + K(K-1)a = 1 \quad (\text{A6})$$

or

$$a = \frac{1}{K(K+1)}. \quad (\text{A7})$$

Thus,

$$E\{|\tilde{\mathbf{u}}_1' \tilde{\mathbf{v}}_1|^2\} = \|\tilde{\mathbf{u}}_0\|^2 \|\tilde{\mathbf{v}}_0\|^2 \left\{ |\rho|^2 \left[ 1 - \frac{2}{K} + \frac{1}{K(K+1)} \right] + (1 - |\rho|^2) \frac{1}{K(K+1)} \right\}. \quad (\text{A8})$$

Equation (35) follows directly from Eq. (A8).

We now derive Eq. (36). From Eqs. (33) and (34)

$$\begin{aligned} \|\tilde{\mathbf{u}}_1\|^2 \|\tilde{\mathbf{v}}_1\|^2 = \|\tilde{\mathbf{u}}_0\|^2 \|\tilde{\mathbf{v}}_0\|^2 & \left[ 1 - \frac{|y_1|^2}{\mathbf{y}'\mathbf{y}} - \frac{|\rho^* y_1 + \sqrt{1 - |\rho|^2} y_2|^2}{\mathbf{y}'\mathbf{y}} \right. \\ & \left. + \frac{|\rho y_1|^2 + \sqrt{1 - |\rho|^2} y_1^* y_2|^2}{(\mathbf{y}'\mathbf{y})^2} \right]. \end{aligned} \quad (\text{A9})$$

Now the expectations of the individual terms of Eq. (A9) can be evaluated by using some of the previous results.

$$E \left\{ \frac{|y_1|^2}{\mathbf{y}'\mathbf{y}} \right\} = \frac{1}{K}, \quad (\text{A10})$$

$$E \left\{ \frac{|\rho^* y_1 + \sqrt{1 - \rho^2} y_2|^2}{\mathbf{y}'\mathbf{y}} \right\} = |\rho|^2 E \left\{ \frac{|y_1|^2}{\mathbf{y}'\mathbf{y}} \right\} + (1 - |\rho|^2) E \left\{ \frac{|y_2|^2}{\mathbf{y}'\mathbf{y}} \right\}, \quad (\text{A11})$$

$$= |\rho|^2 \frac{1}{K} + (1 - |\rho|^2) \frac{1}{K},$$

$$= \frac{1}{K},$$

and

$$E \left\{ \frac{|\rho |y_1|^2 + \sqrt{1 - \rho^2} y_1^* y_2|^2}{(\mathbf{y}'\mathbf{y})^2} \right\} \quad (\text{A12})$$

$$\begin{aligned}
&= |\rho|^2 E \left\{ \frac{|y_1|^4}{(\mathbf{y}'\mathbf{y})^2} \right\} + (1 - |\rho|^2) E \left\{ \frac{|y_1|^2 |y_2|^2}{(\mathbf{y}'\mathbf{y})^2} \right\}, \\
&= |\rho|^2 \frac{2}{K(K+1)} + (1 - |\rho|^2) \frac{1}{K(K+1)}, \\
&= \frac{1}{K(K+1)} (1 + |\rho|^2).
\end{aligned}$$

Thus,

$$E\{\|\tilde{\mathbf{u}}_1\|^2 \|\tilde{\mathbf{v}}_1\|^2\} = \|\tilde{\mathbf{u}}_0\|^2 \|\tilde{\mathbf{v}}_0\|^2 \left[ 1 - \frac{2}{K} + \frac{1}{K(K+1)} (1 + |\rho|^2) \right]. \quad (\text{A13})$$

Equation (36) follows from Eq. (A13).